AB569, a nontoxic chemical tandem that kills major human pathogenic bacteria

Cameron T. McDaniel[a], Warunya Panmanee[a], Geoffrey L. Winsor[b], Erin Gill[c], Claire Bertelli[b], Michael J. Schurr[d], Prateek Dongare[e], Andrew T. Paul[a], Seung-Hyun B. Ko[a], Gee W. Lau[f], Nupur Dasgupta[g], Amy L. Bogue[a], William E. Miller[a], Joel E. Mortensen[h], David B. Haslam[i], Phillip Dexheimer[g], Daniel A. Muruve[j], Bruce J. Aronow[g], Malcolm D. E. Forbes[k], Marek Danilczuk[k], Fiona S. L. Brinkman[b], Robert E. W. Hancock[c], Thomas J. Meyer[e,1], and Daniel J. Hassett[a,1]

[a]Department of Molecular Genetics, Biochemistry and Microbiology, University of Cincinnati College of Medicine, Cincinnati, OH 45267; [b]Molecular Biology and Biochemistry, Simon Fraser University, Burnaby, BC V5A 1S6, Canada; [c]Centre for Microbial Diseases and Immunity Research, Department of Microbiology and Immunology, University of British Columbia, Vancouver, BC V6T 1Z3, Canada; [d]Department of Microbiology and Immunology, University of Colorado at Denver, Aurora, CO 80045; [e]Department of Chemistry, University of North Carolina at Chapel Hill, Chapel Hill, NC 27599; [f]College of Veterinary Medicine, University of Illinois at Urbana–Champaign, Urbana, IL 61802; [g]Computational Medicine Center, Cincinnati Children's Hospital Medical Center, Cincinnati, OH 45229; [h]Diagnostic and Infectious Disease Testing Laboratory, Department of Pathology and Laboratory Medicine, Cincinnati Children's Hospital Medical Center, Cincinnati, OH 45229; [i]Department of Pediatrics, Cincinnati Children's Hospital Medical Center, Cincinnati, OH 45229; [j]Department of Medicine, University of Calgary, Calgary, AB T2N4Z6, Canada; and [k]Center for Photochemical Studies, Bowling Green State University, Bowling Green, OH 43403

Contributed by Thomas J. Meyer, December 30, 2019 (sent for review July 15, 2019; reviewed by Benjamin Gaston and Niels Høiby)

Antibiotic-resistant superbug bacteria represent a global health problem with no imminent solutions. Here we demonstrate that the combination (termed AB569) of acidified nitrite (A-NO_2^-) and Na_2-EDTA (disodium ethylenediaminetetraacetic acid) inhibited all Gram-negative and Gram-positive bacteria tested. AB569 was also efficacious at killing the model organism *Pseudomonas aeruginosa* in biofilms and in a murine chronic lung infection model. AB569 was not toxic to human cell lines at bactericidal concentrations using a basic viability assay. RNA-Seq analyses upon treatment of *P. aeruginosa* with AB569 revealed a catastrophic loss of the ability to support core pathways encompassing DNA, RNA, protein, ATP biosynthesis, and iron metabolism. Electrochemical analyses elucidated that AB569 produced more stable SNO proteins, potentially explaining one mechanism of bacterial killing. Our data implicate that AB569 is a safe and effective means to kill pathogenic bacteria, suggesting that simple strategies could be applied with highly advantageous therapeutic/toxicity index ratios to pathogens associated with a myriad of periepithelial infections and related disease scenarios.

bactericidal | sodium nitrite | EDTA | biofilm | antibiotic resistance

Cystic fibrosis (CF) and chronic obstructive pulmonary disease (COPD) are both pulmonary disorders characterized in part by the presence of chronic airway infections. These are often associated with multidrug-resistant pathogens such as *Pseudomonas aeruginosa* (PA), *Acinetobacter baumannii*, and *Staphylococcus aureus*, leading to diminishing efficacy in available treatments as the patient ages. In 2006, we showed that acidified nitrite (A-NO_2^-) is a powerful bactericidal agent against the antibiotic and phagocyte refractory mucoid form of PA, often associated with CF and COPD, killing both planktonic and biofilm bacteria with no adverse effects on human airway cells (1). We subsequently showed that A-NO_2^- also kills two other major CF pathogens, *S. aureus* and *Burkholderia cepacia* (2). The nitric oxide (NO) derived from A-NO_2^- reduction binds to Fe-S cluster proteins and heme, forming dinitrosyliron complexes (3), but also to nonheme iron, copper, and reactive thiols (4). NO also reduces *lpdA* transcription (encoding lipoamide of the pyruvate dehydrogenase, PDH) by 50%, via α-ketoglutarate dehydrogenase and PDH in *S. aureus* (5). A similar effect on iron metabolism and processing is also triggered by chelators such as EDTA (ethylenediaminetetraacetic acid), which also triggers dispersion of bacteria embedded in biofilms (6). However, EDTA also perturbs bacterial membranes and chelates Ca^{2+} and Mg^{2+} in lipopolysaccharide (LPS), thereby further taxing the bacterial outer membrane by allowing significant LPS release (7). EDTA is also synergistic with multiple antibiotics in bacterial killing (8), including in a canine model (9), although it should be noted that the use of EDTA in pulmonary treatments is contested due to bronchoconstriction seen following the use of nebulized calcium chelators (10–12).

In this study, we report the unexpected finding of the synergistic killing of many Gram-negative (G–) and additive killing of

Significance

Currently, the number of medical cases associated with antibiotic-resistant bacteria is increasing at a staggering pace. Antibiotic development is not keeping pace with this rise, leading to a desire for new and alternative methods to treat infections. This report focuses on the ability of EDTA (ethylenediaminetetraacetic acid) and sodium nitrite (two simple, inexpensive, and widely available compounds) to act in a combinatorial fashion to inhibit and kill a variety of clinically relevant bacteria. The known individual effects of each compound were evaluated in the combination, examining how the combination provides this increased microbial inhibition and killing. Additionally, this combination was safe at higher dosages in a mouse model, indicating its potential as a human therapeutic agent.

Author contributions: C.T.M., G.L.W., E.G., M.J.S., P. Dongare, G.W.L., W.E.M., B.J.A., M.D.E.F., M.D., F.S.L.B., T.J.M., and D.J.H. designed research; D.J.H. was project leader; C.T.M., W.P., G.L.W., E.G., C.B., M.J.S., P. Dongare, A.T.P., S.-H.B.K., G.W.L., N.D., A.L.B., J.E.M., P. Dexheimer, B.J.A., M.D.E.F., M.D., T.J.M., and D.J.H. performed research; G.L.W., E.G., P. Dongare, G.W.L., W.E.M., J.E.M., D.B.H., B.J.A., M.D.E.F., M.D., F.S.L.B., and R.E.W.H. contributed new reagents/analytic tools; C.T.M., W.P., G.L.W., E.G., C.B., M.J.S., P. Dongare, G.W.L., N.D., W.E.M., P. Dexheimer, D.A.M., B.J.A., M.D.E.F., M.D., F.S.L.B., R.E.W.H., T.J.M., and D.J.H. analyzed data; and C.T.M., G.L.W., and D.J.H. wrote the paper.

Reviewers: B.G., Case Western Reserve University and Rainbow Babies and Children's Hospital; and N.H., Rigshospitalet.

Competing interest statement: D.J.H. is a lead scientist for Arch Biopartners and has a US patent on AB569 (9,925,206) issued on March 27, 2019. D.A.M. is a cofounder and Chief Science Officer for Arch Biopartners. Arch Biopartners owns an exclusive option to license with the University of Cincinnati any patents regarding AB569.

Data deposition: The RNA sequencing results have been uploaded to the National Center for Biotechnology Information Gene Expression Omnibus database (https://www.ncbi.nlm.nih.gov/geo) and can be accessed with series entry number GSE142611.

[1]To whom correspondence may be addressed. Email: tjmeyer@unc.edu or daniel.hassett@uc.edu.

This article contains supporting information online at https://www.pnas.org/lookup/suppl/doi:10.1073/pnas.1911927117/-/DCSupplemental.

First published February 18, 2020.

Gram-positive (G+) bacteria tested (including those that are classified as antibiotic-resistant) using the chemical tandem of A-NO_2^- and EDTA (herein termed AB569, in cooperation with Arch Biopartners). The components are biocides that, at relatively low but bactericidally efficacious concentrations, do not affect mammalian cell viability. This relatively simple discovery illuminates a means to potentially help eradicate problematic bacterial biofilm infections, especially those involving antibiotic-resistant organisms in numerous clinical infectious diseases.

Results

AB569 Is Effective Against All Tested G− and G+ Bacteria Under CF Airway Conditions. It must be emphasized that nitrite (NO_2^-) alone at pH values >7.0 may help bacteria capable of anaerobic respiration grow. We have shown that A-NO_2^- can kill clinically problematic antibiotic- and phagocyte-resistant mucoid, *mucA22* mutant *P. aeruginosa* bacteria, at pH 6.3 to 6.5, the pH of the airway surface liquid lining the lungs of CF patients (1, 13). We subsequently showed that a mutant lacking a putative transmembrane-spanning ABC (ATP-binding cassette) transporter permease (PA4455) was also remarkably sensitive to EDTA (14). Thus, we evaluated the antibacterial efficacy of AB569, using those previous concentrations of 1 mM EDTA and 15 mM NO_2^- as benchmark concentrations for this study. Kill curves generated by these treatments indicated more bacterial killing by AB569 at these combination concentrations than either A- NO_2^- or EDTA alone (*SI Appendix*, Fig. S1*A*). We additionally analyzed both *P. aeruginosa* PAO1 and *S. aureus* USA300 in their sensitivity to AB569 in media that did not contain background nitrate (LB 6.5). From these experiments, it appeared that both organisms were still sensitive, yet the combination seemed to act in bacteriostatic pattern aerobically, while functioning as a bactericidal agent anaerobically (*SI Appendix*, Fig. S1 *B–E*). Next, the checkerboard method of sensitivity testing was used to determine the concentrations that are effective for each chemical independently (minimum inhibitory concentrations [MICs] or combined fractional inhibitory concentrations [FICs]) (15, 16). This assay allows for the determination of the FIC index, an indicator of synergy, via the equation $FIC_{Index} = (FIC_A/MIC_A) + (FIC_B/MIC_B)$. If the result of the two fractions is less than 0.5, the combination is considered synergistic. If the result is between 0.5 and 1.0, the combination can be considered weakly synergistic (17). Otherwise, 1.0 to 4.0 is considered additive, and 4.0+ is antagonistic. This technique allows for the assessment of a breadth of concentrations to determine bacterial sensitivity. We first tested the efficacy of EDTA against aerobic wild-type *P. aeruginosa* PAO1, in comparison to A-NO_2^- in LBN 6.5. Surprisingly, we found that the combination of the two led to significantly enhanced growth inhibition with a calculated FIC_{Index} of 0.25.

To test the antimicrobial breadth of AB569, 18 total G− and G+ bacteria were used in checkerboard experiments to determine MICs of A-NO_2^- or EDTA and FICs/FIC_{Index} of AB569 under aerobic and anaerobic conditions depending upon the physiological capabilities of each organism. To maintain as few culture conditions as possible, we focused on those isolates that were able to grow in either Luria–Bertani Broth (LB) or Tryptic Soy Broth (TSB). After checkerboard plate growth for 24 to 48 h, the MICs, FICs, and FIC_{index} values were assessed (Table 1). One strain of ABR *PA* (coined BAMF) was resistant to all tested antibiotics, including colistin, yet it was highly susceptible to AB569, mirroring PAO1 sensitivity. Although AB569 was effective against all bacteria, several G− bacteria revealed a synergistic effect, including *Escherichia coli*, *Klebsiella pneumoniae*, anaerobic *Proteus mirabilis*, and *Salmonella typhimurium*. Additionally, a number of species fell into what has been considered weak synergy ($0.5 < FIC_{index} < 1.0$) (Table 1) (17). Although AB569 also inhibited all G+ bacteria, it was with either weak synergy or an additive effect (Table 1). These results are also shown in the average FIC_{index} for both G− and G+ organisms. G− bacteria fell into the synergy or weak synergy ranges effect, depending on condition (FIC_{index} 0.583 aerobic, 0.431 anaerobic), while the G+ bacteria were solidly within the additive range (FIC_{index} 1.357 aerobic, 1.107 anaerobic). This difference was also statistically significant when comparing across oxygen availability (aerobic $P \leq 0.002$, anaerobic $P \leq 0.02$). As indicated, a vast number of organisms could be inhibited with far less than the benchmark concentrations of 15 mM $NaNO_2$ and 1 mM EDTA.

NO_2^- and EDTA Trigger Dispersion and Killing of Bacterial Biofilms. While the ability of AB569 to kill planktonic bacteria was encouraging, we were also interested in its effect on established biofilms, a form of growth that has been estimated to compose over 80% of all infections (18). Therefore, we focused on the biofilm forming ability of two major pathogens known for antibiotic resistance, *PA* PAO1 and *S. aureus* USA300, a known methicillin-resistant strain (Fig. 1). Biofilms were grown for 24 h in both aerobic and anaerobic conditions. After 48 h of treatment with A-NO_2^- and/or EDTA at different concentrations, we removed the media and used FACS analysis coupled with a Syto9/propidium iodide viability stain to assess the killing efficacy of each compound alone or AB569. The fold differences of live cells (white bars) and dead cells (black bars) as compared to untreated bacterial biofilms were calculated and plotted. These data in Fig. 1 indicate that A-NO_2^-, EDTA, and especially AB569 are effective at killing biofilm bacteria, although once again the trend favors the killing of the G− *PA* PAO1.

Transcriptional Profiling of Anaerobic *PA* PAO1 Treated with AB569: Genetic Responses. While the inhibition and killing data are translationally promising, the mechanism of the synergistic killing in G− bacteria was unclear. To help address this critical mechanism, an RNA-seq approach was utilized. Anaerobically grown (representing chronic CF airway disease; ref. 19) *PA* PAO1 were treated with the AB569 components (A-NO_2^- and/or EDTA) with either or both of the compounds at benchmark concentrations, and RNA was extracted. The relative abundance of transcripts was determined, and differentially expressed genes with a cutoff of 1.5-fold as compared to the untreated control were selected for further analysis (20). The comparative overview of enriched biological processes Gene Ontology (GO) terms is presented in Fig. 2, with the processes indicated under the condition in which they were enriched.

Metabolic Pathway/GO Overrepresentation Analysis. We used three complementary approaches for overrepresentation analysis based on KEGG (Kyoto Encyclopedia of Genes and Genomes) pathways (GAGE [Generally Applicable Gene-Set Enrichment] software), PseudoCyc metabolic pathways, and GO term annotations. For analysis, the focus was placed on PseudoCyc metabolic pathways and GO biological processes annotations. The results for each approach showed notable similarities that added more confidence to our presented results, given that each of the three methods have their own biases.

Down-Regulation of Key Vital Pathways by AB569 Treatment. A comparison of the three treatments investigated in this study, based on PseudoCyc analysis, revealed that bacteria treated with AB569 led to down-regulation of the highest proportion of genes belonging to biosynthetic pathways (188 genes vs. 170 genes or 123 genes down-regulated by A-NO_2^- or EDTA treatment, respectively) and degradation pathways (59 genes vs. 50 genes or 32 genes down-regulated by A-NO_2^- or EDTA treatment, respectively) (*SI Appendix*, Table S1). Gene enrichment analysis using KEGG/GAGE analysis found that AB569 induced down-regulation of the same pathways observed with the other treatments (with the exception of the general metabolic superpathways

Table 1. A comprehensive list of bacteria that have been subjected to AB569 sensitivity testing using the checkerboard method of synergy

Media	Bacteria	Oxygen +\–	MIC (mM)		FIC (mM)			
			NO_2^-	EDTA	NO_2^-	EDTA	FIC_{index}	Classification
Gram negative								
LBN 6.5	*Enterobacter cloacae*	+	32	>16	16	0.5	<0.53	Weak synergy
		–	32	16	16	0.5	0.53	Weak synergy
LBN 6.5	*E. coli*	+	64	16	16	0.5	0.28	Synergy
		–	32	>16	8	0.5	<0.28	Synergy
LBN 6.5	*K. pneumoniae*	+	64	16	4	2	0.19	Synergy
		–	64	>16	16	0.5	<0.28	Synergy
LBN 6.5	*P. aeruginosa* (PAO1)	+	32	2	8	0.5	0.50	Weak synergy
		–	16	1	2	0.5	0.63	Weak synergy
LBN 6.5	MDR–*P. aeruginosa* BAMF	+	32	4	8	1	0.50	Weak synergy
		–	16	1	4	0.5	0.75	Weak synergy
LBN 6.5	*P. mirabilis*	+	64	1	16	0.5	0.75	Weak synergy
		–	64	2	2	0.5	0.28	Synergy
LBN 6.5	*S. typhimurium*	+	64	>16	16	0.5	<0.28	Synergy
		–	64	>16	16	0.25	<0.27	Synergy
TSBN 6.5	*Acinetobacter baumanii*	+	16	1	8	0.25	0.75	Weak synergy
LBN 6.5	*Burkholderia cepacia*	+	16	2	8	1	1.00	Additive
LBN 6.5	*Ralstonia* sp.	+	8	0.5	1	0.25	0.63	Weak synergy
TSBN 6.5	*Stenotrophomonas maltophila*	+	16	0.5	8	0.25	1.00	Additive
Gram positive								
LBN 6.5	*Bacillus* sp.	+	32	0.25	32	0.25	2.00	Additive
		–	8	0.25	8	0.25	2.00	Additive
TSBN 6.5	*Corynebacterium* sp.	+	16	1	16	1	2.00	Additive
		–	32	0.5	32	0.5	2.00	Additive
LBN 6.5	*Enterococcus faecalis*	+	>64	1	32	0.5	<1.00	Weak synergy
		–	32	2	16	1	1.00	Additive
LBN 6.5	*Enterococcus faecium*	+	64	0.5	16	0.25	0.75	Weak synergy
		–	64	0.5	16	0.25	0.75	Weak synergy
TSBN 6.5	*Listeria monocytogenes*	+	32	0.5	32	0.5	2.00	Additive
		–	32	1	8	0.25	0.50	Additive
LBN 6.5	*Staphylococcus aureus* (USA300)	+	64	0.5	32	0.25	1.00	Additive
		–	32	1	4	0.5	0.75	Weak synergy
LBN 6.5	*Staphylococcus epidermidis*	+	64	4	16	2	0.75	Weak synergy
		–	16	0.5	4	0.25	0.75	Weak synergy

observed after treatment with A-NO_2^-) along with several unique pathways (*SI Appendix*, Table S2). All conditions triggered a significant down-regulation of ribosomal synthesis genes and those involved in bacterial secretion. AB569 and A-NO_2^- treatment shared four other pathways, notably protein export and biosynthesis of amino acids. However, AB569 exhibited several unique down-regulated pathways, including homologous recombination, purine metabolism, aminoacyl-tRNA biosynthesis, biosynthesis of antibiotics, and several others. GO term overrepresentation analysis also identified secretion, type IV pilus biogenesis, and the critical tRNA aminoacylation/charging step associated with translation (Fig. 3), supporting the above KEGG/GAGE analysis as being enriched terms from down-regulated genes of only the AB569-treated cells (*SI Appendix*, Table S3). These unique and common pathways suggest an overall dysfunction of DNA and protein synthesis under AB569 conditions, processes that are critical for viability and to be able to mount a defense against nitrosative stress.

After observing the down-regulation of several genes related to viability, we investigated the effect of AB569 exposure on all genes that are essential for *PA* survival, as determined by the complete list of genes that do not have transposon insertions from a previously described PAO1 Tn*5-luxCDABE* mutant library (21). We determined that 236 essential genes with lengths ≥300 bp were down-regulated upon treatment with AB569. To ascertain the biological processes in which these genes are involved, enrichment analysis was performed with GAGE using KEGG annotations as described above. The enriched down-regulated pathways include ribosome (q value = 1.35E-03), metabolic pathways (q value = 1.23E-02), biosynthesis of antibiotics (q value = 2.95E-02), pyrimidine metabolism (q value = 3.93E-02), biosynthesis of secondary metabolites (q value = 4.32E-02), and carbon metabolism (q value = 4.32E-02). Not surprisingly, the vast down-regulation of these essential genes would prove problematic for PAO1.

Up-Regulation of Key Pathways during AB569 Treatment. Similar to the down-regulated genes, AB569 was also responsible for the greatest up-regulation of genes in the biosynthetic pathways class (62 genes vs. 57 genes or 54 genes up-regulated by A-NO_2^- or EDTA treatment, respectively) and degradation pathways (65 genes vs. 56 genes for both A-NO_2^- and EDTA treatments), as demonstrated from the PseudoCyc pathway analysis (*SI Appendix*, Table S1). GO term overrepresentation analysis performed on the up-regulated genes identified 23 enriched biological processes that were significantly enriched (compared to 29 due to EDTA and 23 to A-NO_2^- treatments), including phosphorelay signal transduction systems (two-component signaling), regulation of single-species biofilm formation, and iron-sulfur cluster assembly that were among five pathways enriched only by AB569 treatment (Fig. 3 and *SI Appendix*, Table S4). However, when examining the common pathways up-regulated by all conditions,

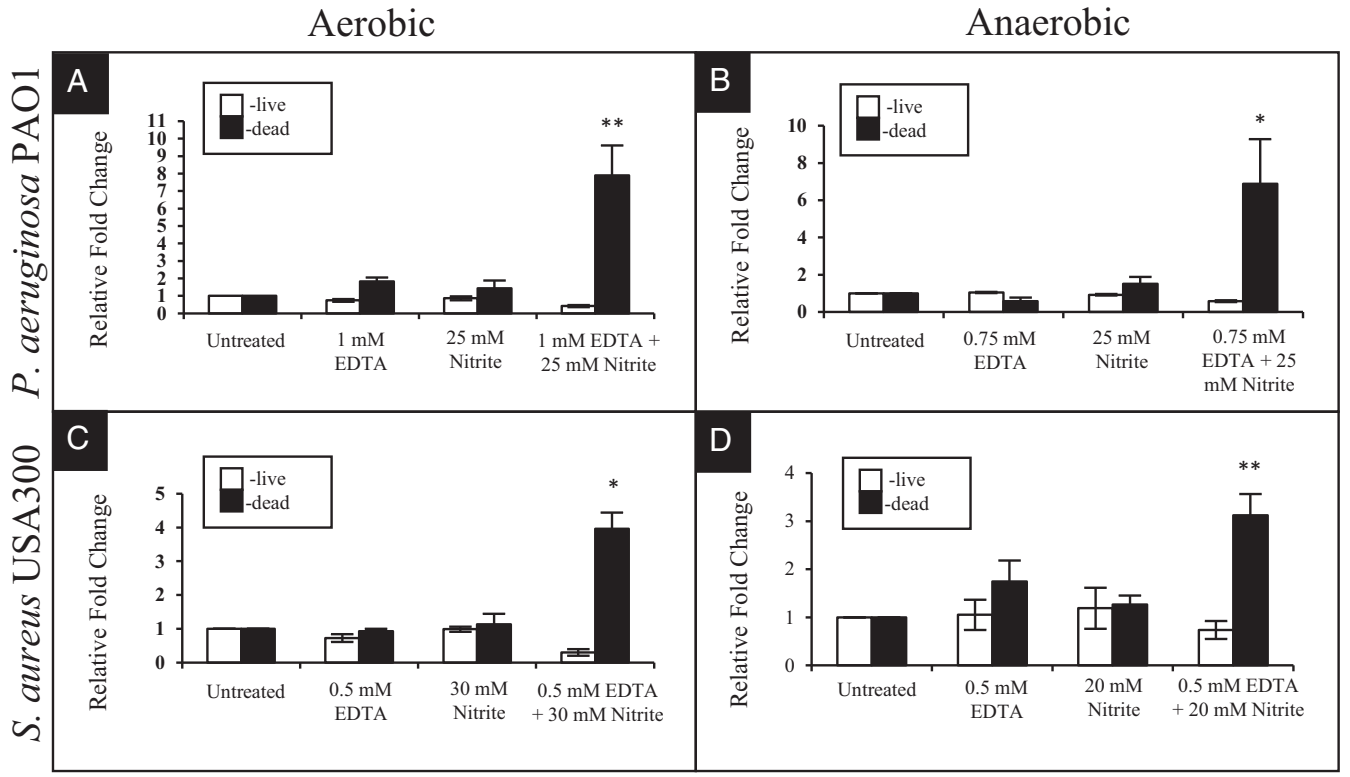

Fig. 1. Killing of biofilm bacteria by AB569. (*A* and *B*) *PA* PAO1 and (*C* and *D*) *S. aureus* USA300 were used to grow aerobic (*A* and *C*) and anaerobic (*B* and *D*) biofilms for 24 h, followed by treatment with either A-NO_2,EDTA, or AB569 for 48 h. Following PBS washes, cells were resuspended, stained with a BacLight live/dead stain, and analyzed via flow cytometry. The changes in gated live (white bars) and dead (black bars) cells were calculated and plotted. The greatest increase in dead cells was associated with AB569 in all cases. (**$P < 0.01$ and *$P < 0.05$.)

iron-related pathways were predominant (including siderophore transport, regulation of iron ion transport, ferric iron transport, and iron coordination entity transport). Given the ability of both A-NO_2^- and EDTA to affect available iron pools (notably through formation of DNICs, chelation of extracellular metal), it is not surprising that these pathways dominated the common up-regulated pathways for all conditions. Perhaps more surprising was the disproportionate response of the bacteria in the production of pyoverdine and pyochelin siderophore genes. Upon further investigation into the up-regulation of these siderophore biosynthetic pathways, it became apparent that the EDTA treatment was up-regulated at a disproportionate ratio to A-NO_2^- and AB569. Pyoverdine biosynthesis was enriched under all three conditions, yet levels in EDTA-treated organisms were ∼100-fold higher (*SI Appendix*, Fig. S2). This was accompanied by a 115-fold increase in transcription of *pvdS* (*SI Appendix*, Fig. S3), a positive regulator of pyoverdine biosynthesis. Analysis of pyochelin biosynthesis gene expression in EDTA-treated bacteria revealed an ∼50-fold or greater increase in transcription of the ferripyoverdine receptor gene, *fptA*; its regulatory gene, *pchR*; and a ferripyoverdine transporter gene, *fptX* (*SI Appendix*, Fig. S3).

Cyclic Voltammetry Electrochemical Analysis of AB569. Given the increased efficacy of AB569 compared to A-NO_2^- treatment alone, we proposed that AB569 may increase the amount of NO produced during treatment, leading to this effect. Several electrochemical assays were employed that can detect the nitrosyl radical. The first was cyclic voltammetry, which is known to detect redox reactions/intermediates through the application and removal of a reducing potential, resulting in the reduction and oxidation of the system. Of note, the Fe(NO^+)/Fe($NO^•$) species have been reported to appear at Ep = −800 mV in similar studies using model complexes as well as biological samples (22). To perform the analysis in a relevant media, cyclic voltammetry (CV) was performed in modified LBN 6.5 with 0.2 M NaCl as the electrolyte. Upon addition of 15 mM $NaNO_2$ to the modified LBN 6.5, an irreversible peak at Ep = −800 mV appeared (Fig. 3*A*). This same peak was not observed when 0.5 mM EDTA was added (Fig. 3*B*). However, when EDTA plus $NaNO_2$ were mixed together and the CV was acquired, an irreversible peak at Ep = −800 mV appeared (Fig. 3*C*). This indicates the putative formation of an $NO^•$ species at a relatively greater extent when EDTA and $NaNO_2$ were mixed. Based on the aforementioned observations, a reasonable interpretation is the formation of a redox active species that resembles NO^+/$NO^•$ pair when EDTA and $NaNO_2$ are mixed together.

Amperometric Detection of NO Produced by AB569 and Individual Components. Amperometric detection was also used to allow for detection of low concentrations (∼1 nM) of NO produced from either nitrite, EDTA, or AB569 minus bacteria. As expected, the addition of 1 mM EDTA alone did not elicit a significant change in baseline. However, nitrite and AB569 were able to produce detectable amperage changes. As depicted from a representative trial (Fig. 3*D*), the peaks of NO production between $NaNO_2$ plus EDTA (left) and $NaNO_2$ only (right) were similar, even following excess nitrite addition. This suggested that the addition of EDTA did not increase the amount of NO being produced on a purely chemical basis. However, this would not necessarily rule out the interaction of NO with other biomolecules, leading to the formation of dinitrosyl iron complexes (DNICs) and NO-containing molecules that can be detected via additional means.

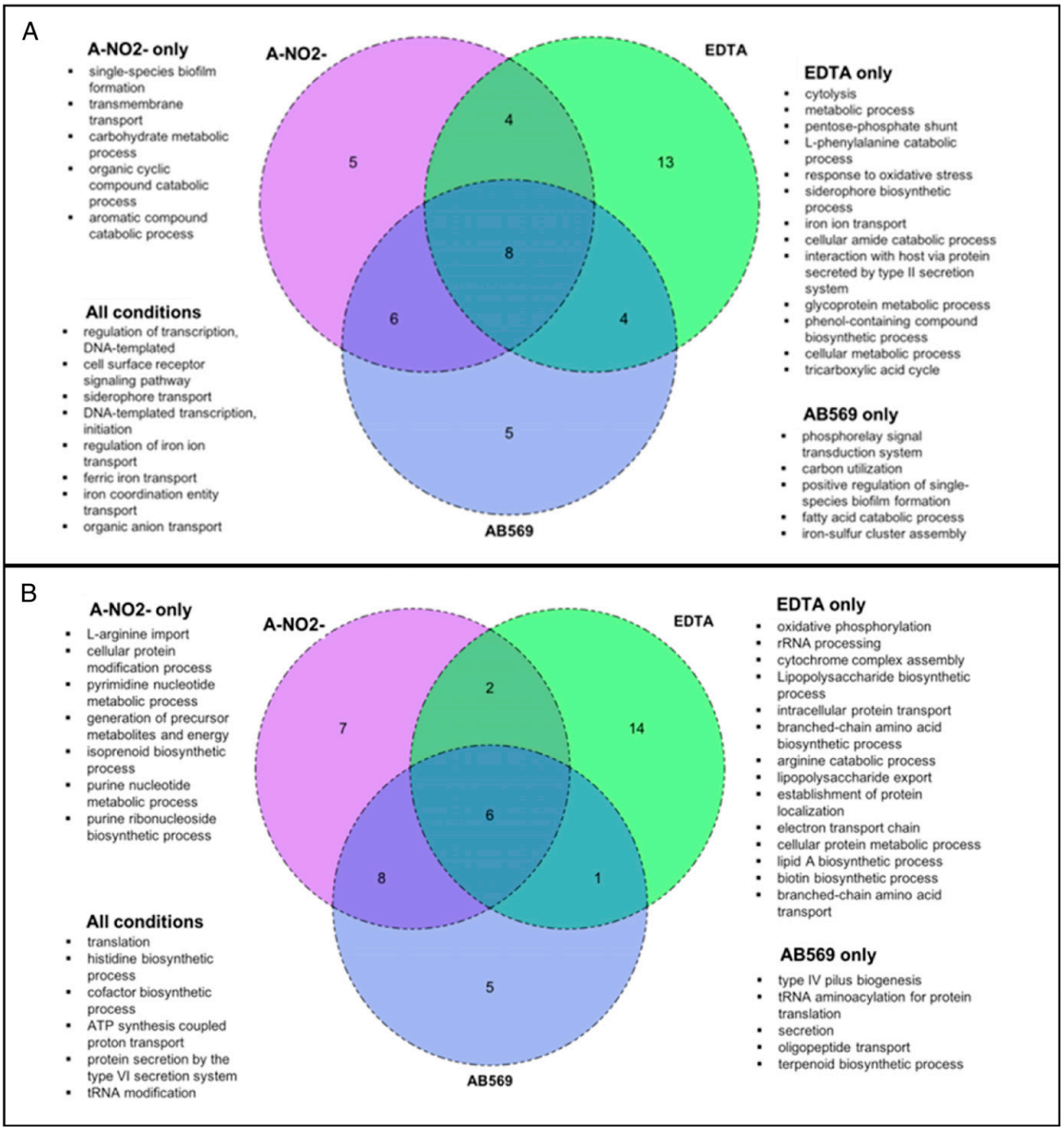

Fig. 2. Summary of Gene Ontology (GO) terms for biological processes that were enriched from sets of (*A*) up-regulated and (*B*) down-regulated *PA* PAO1 genes following treatment with A-NO_2^-, EDTA, or AB569. Terms that were enriched under only one condition are listed under the heading of that condition. More comprehensive breakdowns in pathway expression can be found in *SI Appendix*, Tables S1–S4 and Figs. S2 and S3.

Electron Paramagnetic Resonance Analysis of AB569. Finally, we employed electron paramagnetic resonance (EPR) spectroscopy in our search for the chemical underpinnings of the AB569 antibacterial mechanism. EPR detects unpaired electrons in samples through their magnetic moments and interactions with nearby nuclei, allowing for unique spectra depending on the species in question. Historically, EPR has been a prime assay to investigate a variety of DNICs. Although it is possible to discern the various DNICs apart to some degree based on variations of peak measurements ($g \sim 2.03$, based on bound R-group) (23, 24), it was decided that this would be difficult in the complex media of LBN 6.5. Instead, iron-*N*-methyl-D-glucamine dithiocarbamate (MGD-Fe) (25) was utilized, a well-known spin trap for NO that produces an EPR-detectable 1:1:1 triplet. We focused on concentrations of 15 mM $NaNO_2$ and 1 mM EDTA in LBN 6.5 to mimic earlier bactericidal testing to determine if detectable NO is produced by the appearance of this MGD-Fe triplet. The MGD spin adduct was detected only in the added $NaNO_2$ condition (black line) but

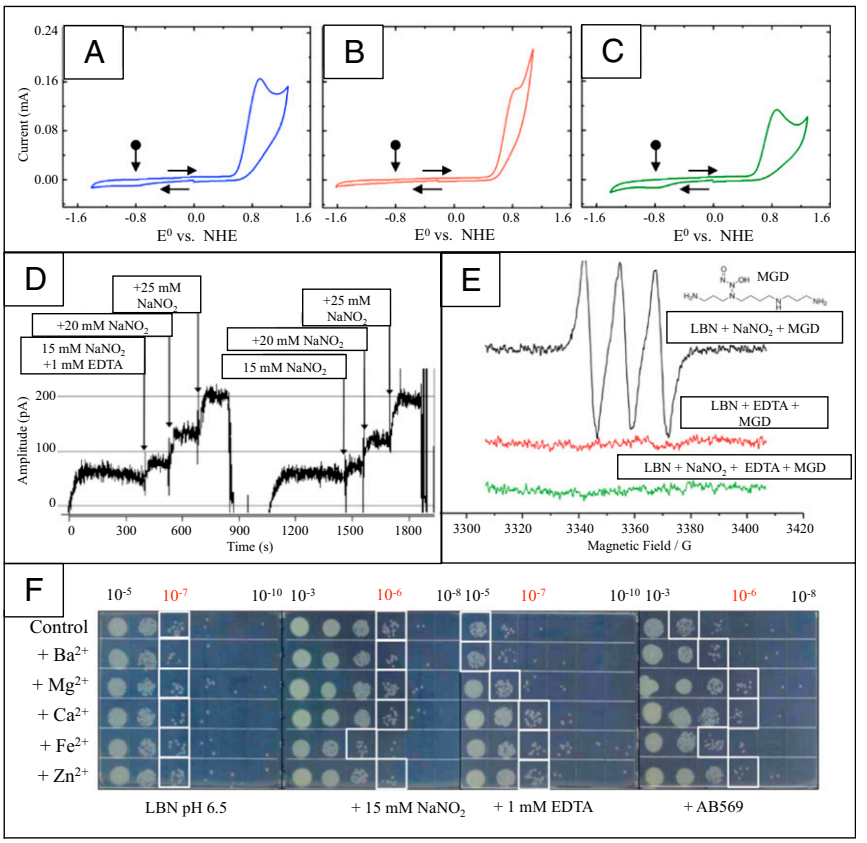

Fig. 3. Electrochemical analyses of AB569. (*A*–*C*) CV of LBN 6.5 (0.2 M NaCl) + 15 mM $NaNO_2$ (*A*), LBN 6.5 (0.2 M NaCl) + 0.5 mM EDTA (*B*), and LBN 6.5 (0.2 M NaCl) + 0.5 mM EDTA + 15 mM nitrite (*C*) at a scan rate of 100 mV/s. A constant ionic strength is maintained with NaCl (0.2 M) at 295 ± 3 K on a glassy carbon supporting electrode. Horizontal arrows indicate the scan direction. Vertical, ball-ended arrow at −800 mV representing typical $Fe(NO^+)/Fe(NO^•)$ peak. (*D*) Amperometric detection of NO production during the addition of (*Left*) EDTA plus $NaNO_2$ or (*Right*) $NaNO_2$ alone to LBN 6.5 media. Panels indicate concentration of additives. (*E*) EPR detection of NO production using the MGD-Fe spin trap in LBN 6.5 plus 15 mM $NaNO_2$ (black line) or 1 mM EDTA (red line), or both (green line) after 3 h incubation aerobically at 37 °C. (*F*) Treatment of *PA* PAO1 anaerobically with 15 mM $NaNO_2$ and/or 1 mM EDTA for 24 h in the presence of 1 mM of the indicated metal. The experiments were performed at least three times. Plate scans of a representative experiment are shown, with squares indicating the dilutions containing more than 10 CFU.

not in EDTA (red line) or combined conditions (green line) (Fig. 3*E*).

Recovery of *PA* from AB569 Treatment by Divalent Metals. Given that AB569 showed a synergistic interaction with some G− bacteria and weakly synergistic with some G+ bacteria, we posited that a phenotypic difference between the two could be at the root of this phenomenon. The most obvious interaction was the EDTA component with G− membranes, hinging on the availability of Ca^{2+} and Mg^{2+} that are integral linkers of the essential LPS chains. We treated anaerobic *PA* PAO1 with AB569 or individual components, also supplementing the media with divalent metals that have a lesser or greater affinity with EDTA than Ca^{2+} and Mg^{2+}. By adding a metal with a lower affinity (e.g., Ba^{2+}), the cells should still be susceptible to EDTA as it would still preferentially bind Ca^{2+} and Mg^{2+}. Conversely, EDTA should preferentially bind an added metal with a higher affinity (Fe^{2+} and Zn^{2+}), reducing the effect on the cell membrane. To answer if this effect occurred by AB569 treatment, we employed a broth-based killing assay. *PA* PAO1 was incubated with 15 mM $NaNO_2$ and/or 1 mM EDTA in LBN 6.5 anaerobically for 24 h with or without an additional 1 mM of either $BaCl_2$, $MgCl_2$, $CaCl_2$, $FeCl_2$, or $ZnCl_2$. Samples were serially diluted and spotted on plates for CFU enumeration. The resulting growth indicated that the predicted effect of the EDTA component of AB569 could be reversed (Fig. 3*F*). The CFU/mL of the EDTA treated cells resembled untreated conditions after the addition of Ca^{2+} or higher-affinity metal (2 $\log_{10}$ recovery). Metal addition did not affect $NaNO_2$-treated cells. Instead, we only observed a slight increase in killing when cells were treated with Fe^{2+} plus $NaNO_2$. Akin to EDTA treatment, AB569-treated cells showed some level of recovery in the presence of Mg^{2+}, Ca^{2+}, Fe^{2+}, or Zn^{2+} (2 $\log_{10}$ recovery) or Ba^{2+} (1 $\log_{10}$ recovery). However, the CFU/mL only recovered to a quantity mirroring $NaNO_2$ treatment levels. As such, metal addition could reverse the impact of EDTA on the cell membrane but did not affect the impact of $NaNO_2$, suggesting any synergistic effect could not be attributed to the cell membrane.

EDTA Offers Protective Effects to Cys-NO Proteins in Media. NO is known to interact with proteins through nitrosylation, a common form being sulfur nitrosylation, resulting in *S*-nitrosylated (SNO) proteins. SNO proteins can further react with transition metals to produce radicals, either NO or other intermediates. Previous reports on the production of SNO proteins for analytical purposes have noted that a chelator needs to be added to the system (e.g., EDTA) to prevent the reaction of SNO protein with the environmental metal, or the sample is quickly lost. We posited that AB569 might be producing SNO proteins that are protected from environmental transition metals more than in A-NO_2^- treatment. To determine this, the presence of EDTA was tested as to whether it could protect preformed S-nitrosylated cysteine (CysNO) from degradation and prevent the release of NO into the

environment (26, 27). The release of NO was analyzed via amperometric detection as described above. The experiment was performed by the addition of CysNO to LBN 6.5 containing a Clark-Type Nitric Oxide Sensor (ISO-NOP, World Precision Instruments) probe, with any resultant amperometric change detected over time. As depicted in Fig. 4*A*, 10 μM Cys-NO was repeatedly injected into LBN 6.5 with or without 1 mM EDTA. The presence of EDTA in LBN 6.5 (Fig. 4*A*, left peaks) resulted in less NO production at each successive injection as compared to LBN 6.5 without EDTA (Fig. 4*A*, right peaks). After initial observation of this phenomenon, the experiment was repeated with a single injection of 25 μM Cys-NO. As shown in Fig. 4*B*, injection of 25 μM Cys-NO in LBN 6.5 resulted in the detection of ∼8.25 μM NO. However, the addition of 1 mM EDTA to LBN 6.5 reduced NO production by 33% (5.5 μM) (Fig. 4*B*). These results indicate that EDTA offers a protective role for SNO proteins, specifically in our media conditions.

AB569 Is Not Toxic to Human Cells at Bactericidal Concentrations. While AB569 kills pathogenic bacteria effectively, the ability for it to not harm human cells was also critical. Previous reports in humans supported the safety of these individual compounds, suggesting the potential to be nontoxic (1, 9). Sytox Orange staining, a dead cell stain, was used as a reagent in these studies. A variety of concentrations of EDTA and/or $NaNO_2$ were tested against bronchial epithelial cells (CFBE and CFBE + WT-CFTR), adult dermal fibroblasts (HDFa), and bladder epithelia (RT4). EDTA (0.5 to 4 mM) and/or $NaNO_2$ (16 to 256 mM) was applied to the cells for 24 h in appropriate media that was adjusted to a pH of 6.5 using 50 mM phosphate buffer.

The results showed that the acidified supplemented media (pH 6.5) alone caused over 20% cell death when plated at a concentration of 100,000 cells per well, which led to a higher background for analysis. However, we believe that promising results were still obtained at bactericidal concentrations, notably our benchmark concentrations and higher. Following these analyses, the treatment concentrations of 1 mM EDTA/32 mM $NaNO_2$ for all cell types were compared to the survival rate of bacterial biofilms (Fig. 2). Of note, these were not the same concentrations, but in all of the cases, cells were exposed to higher concentrations of both EDTA and $NaNO_2$ than used to effectively kill bacteria. The mammalian cell survival rate was at least 30% more than *PA* PAO1 biofilm-related cells and 40% more than *S. aureus* USA300 biofilm cells (Fig. 5*A*).

AB569 Kills *PA* PAO1 during a Chronic Lung Infection in Mice. To test whether AB569 could kill *PA* PAO1 in vivo, we employed an established chronic lung infection model in mice (1). After initial infection, mice were treated twice daily with either 5 mM EDTA/50 mM A-NO_2^- or 10 mM EDTA/100 mM A-NO_2^- in 50 mM PBS (phosphate-buffered saline), pH 6.5. All treatments were administered by nasal inhalation and subsequent intratracheal delivery. Treatments continued for 5 d postinfection after which the mice were then killed. Fig. 5*B* demonstrates that each treatment reduced bacterial titers, with no apparent corresponding histological damage (Fig. 5 *C*–*E*).

Discussion

Bactericidal Activity and Cytotoxicity. As we revealed through both checkerboard assays and broth-based killing assays, AB569 efficacy was not limited to a single species but rather showed broad-spectrum activity against several clinical isolates of different species. Interestingly, the checkerboard results revealed a synergistic effect of AB569 when acting on some G− organisms. Although limited, this was unique to G−s, implying that an aspect of these organisms (such as a pronounced periplasm) may be at the root of this effect. The remaining G− and G+ organisms displayed either weak synergy or an additive effect (Table 1). Given the low doses of both components needed to kill the organisms, we believe this is still acceptable for translational potential. Additionally, the sensitivity of *PA* MDR strain, BAMF, was nearly identical to PAO1. This strain was chosen due to its widespread resistance to antibiotics, including colistin, a contemporary measure of extreme resistance. However, this implies that typical resistance mechanisms cannot defend against AB569 activity. Further testing of biofilm-associated bacteria revealed that AB569 was effective in this manner as well (Fig. 2). This is extremely encouraging as such bacterial macrostructures are increasingly implicated in human disease. This also corroborated initial kill curves generated from planktonic cultures of several strains (*SI Appendix*, Fig. S1*A*). Further testing of PAO1 against AB569 revealed that at least part of the effect of the combination on the bacteria was due to a detrimental effect by EDTA on the bacterial membrane. EDTA is known to chelate Ca^{2+} and Mg^{2+} from the G− membrane, which both weakens the membrane and leaves the cells susceptible to environmental factors. When chelation of Ca^{2+} and Mg^{2+} was in direct competition with metals that have a greater stability complex (Fe^{2+} and Zn^{2+}), the detrimental impact of EDTA on PAO1 was reversed, while the metals seemingly had no impact on rescuing the cells from A-NO_2^- treatment (Fig. 3*F*).

Further cytotoxicity testing was performed on several human cell lines, to show a specificity of toxicity for bacterial treatment. Unfortunately, it appeared that the addition of acidified media to the cells had a somewhat detrimental impact, resulting in ∼20% cell death, slightly more than to be expected for a given population. However, the results indicated that AB569 seemed to slightly increase the survival rate of the HDFa and CFBE ΔF508 cells while having no significant effect on RT4 and CFBE WT-CFTR when compared with pH 6.5 media alone at these concentrations, an unexpected yet encouraging finding. Considering that these are cell monolayers lacking the 3D structure and support of the corresponding tissue, we believed this was an acceptable difference to further pursue in vivo mouse studies to confirm safety of the compounds on healthy tissue. For these

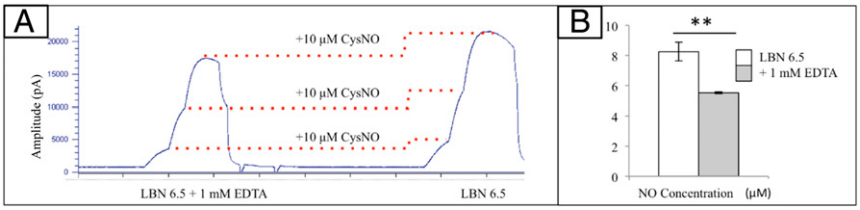

Fig. 4. Amperometric detection of NO released from CysNO in LBN 6.5. (*A*) Representative tracings of the amperometric detection of NO released from CysNO in LBN 6.5 with or without 1 mM EDTA, left peaks and right peaks, respectively. Successive injections of 10 μM occurred ∼30 s apart, and the amplitudes were recorded and compared between conditions. Dotted line indicates equivalent injections between conditions. (*B*) CysNO at 25 μM was injected into LBN 6.5 with or without 1 mM EDTA, and release of NO was quantified. Triplicate experiments were performed, and the amplitude was converted to μM NO using a standard curve (**$P < 0.01$).

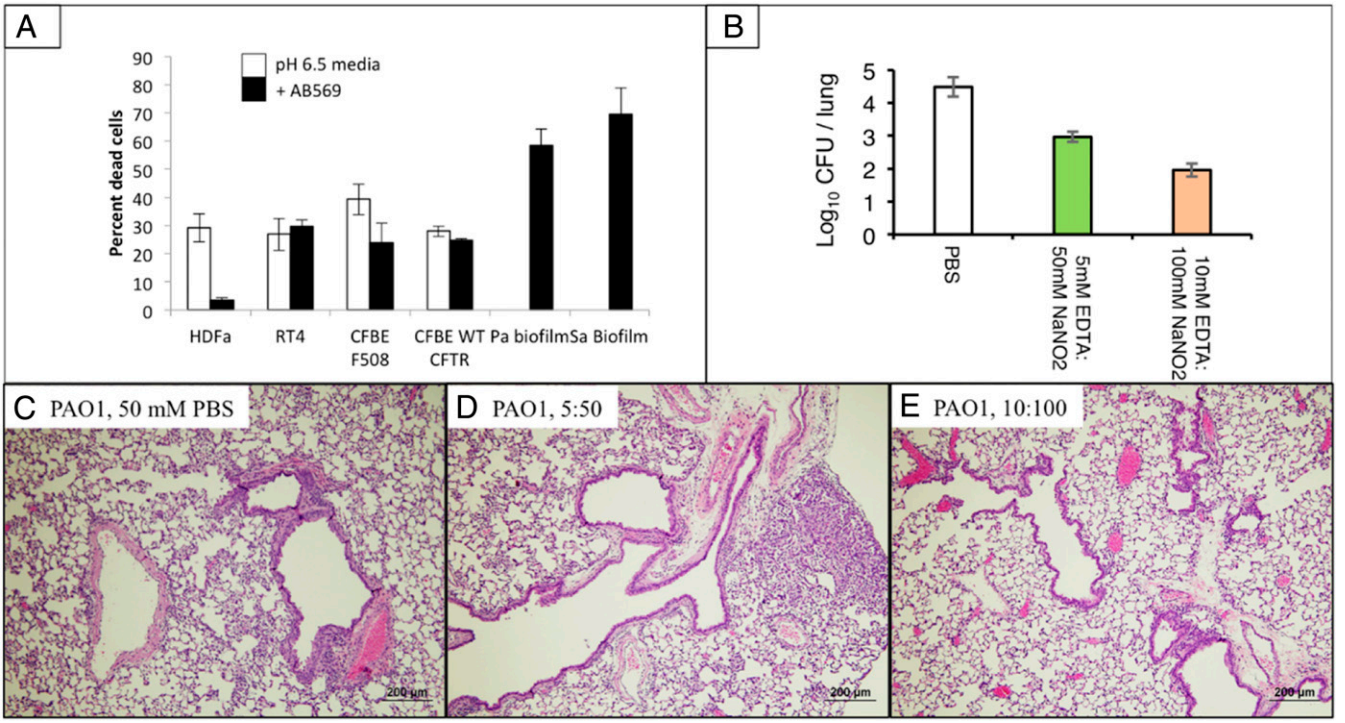

Fig. 5. AB569 is safe and effective for mammalian cells. (*A*) AB569 was tested against several cell types as indicated. At 1 mM EDTA and 32 mM $NaNO_2$, cell viability was determined for CF bronchial epithelia (CFBE, with or without transfected WT CFTR), adult human dermal fibroblasts (HDFa), and bladder epithelia (RT4). Averages of three trials were compared to biofilms treated with similar concentrations of AB569. White bars represent cells treated with media only, while black bars represent cells treated with AB569. (*B*) AB569 at either 5 mM EDTA/50 mM $NaNO_2$ (green bar) or 10 mM EDTA/100 mM $NaNO_2$ (orange bar) in PBS, pH 6.5, was used to treat an in vivo chronic lung infection model in mice, showing a drastic reduction in *PA* PAO1 bacterial load compared to vehicle control (white bar). (*C*–*E*) Corresponding histological studies of treated mice infected with PAO1. Results showed no concomitant histological damage with treatment of either 50 mM PBS (*C*); 5 mM EDTA/50 mM A-NO_2^- in 50 mM PBS, pH 6.5 (*D*); or 10 mM EDTA/100 mM A-NO_2^- in 50 mM PBS, pH 6.5 (*E*). The histopathological analysis was performed independently and in blinded manner by a board-certified anatomic pathologist at the University of Illinois Veterinary Diagnostic Laboratory.

studies, AB569 was delivered intranasally, a process that is known to reduce the effective concentration of a substance once it reaches the lungs. As such, the concentration of AB569 components was increased to ∼5- and 10-fold the set benchmark concentrations. The results were encouraging as they demonstrated that higher concentrations of AB569 could be used and were also corroborative with previous reports on the safety of the individual compounds (1, 9). Additionally, the intranasal treatment, once delivered to the lungs, would be a far lower concentration after travel through the nasal passages. Both nebulization and more frequent dosing will likely need to be a focus in future research using AB569.

Admittedly, more work is needed to understand the effects of AB569 on the eukaryotic cells, both in vitro and in vivo. This study only performed a basic vitality assay for in vitro work and end-point survival and bacterial load enumeration for the in vivo experiment. This then begs several questions on the effect of AB569 on the eukaryotic cells. NO itself has been noted as a carcinogen, which would need to be examined in both cell lines and a mouse model (28, 29). Nitrite and EDTA treatment would also need to be analyzed in in vivo models as to how the treatment would interact with the lungs and how it infiltrates systemically. Additionally, moving into in vivo models should prompt an investigation on the impacts of the treatment on the lung microbiome, both from a homeostatic microbiome standpoint (30, 31) and as it has been recently noted that the microbiome may have a larger impact on host biology through interactions with microRNAs (32). These studies, along with time course and dose–response studies, should be a part of any future investigation into this tandem's effect on eukaryotic cells.

Transcriptomic Alterations. Both EDTA and $NaNO_2$ have a wide variety of effects on cells through several different pathways. Therefore, it was not surprising to see that the PAO1 transcriptome underwent a myriad of changes in response to AB569 treatment. However, included in those changes for AB569-treated cells was the down-regulation of several pathways involving survival, including pyrimidine and carbon metabolism, and ribosomal pathways. If these essential pathways are shut down in response to treatment, it would follow that the cells would begin to perish in response to the NO-based treatment. Further investigation into the exact genes involved in this down-regulation and whether overexpression of them could lead to a protective effect against AB569 is warranted. However, the robust response still speaks volumes to the bactericidal breadth of the combination.

One of the more unexpected aspects discovered was the up-regulation of gene pathways for siderophore production in PAO1 in response to EDTA and AB569 treatment. It is not necessarily surprising that the up-regulation in response to EDTA is so strong, given its chelation ability. In contrast, such a response was not observed in AB569-treated cells (*SI Appendix*, Table S4 and Figs. S3 and S4). Since EDTA is a component of AB569 and would also chelate metals in the extracellular milieu, the lack of robust response could indicate that AB569 treated cells are hampered in their ability to respond to this stress. Considering the wide biological requirement of iron, this could have vast implications on bacterial survival.

Chemical Basis of Action. Despite having seen the drastic effects of AB569 on PAO1 and other bacteria, the exact mechanism of action remained unclear. Genetic analyses of treated cells, while

revealing, were too vast to guide an investigation. The next step was to delve into the potential chemical underpinnings of the combination. While both agents have histories of antimicrobial action, the toxic and radical nature of NO produced from A-NO_2^- would likely have to play a role in the combinations action, perhaps by being produced in greater quantities or existing in a more stable form. To investigate this phenomenon, several electrochemical techniques were used to detect the formation of NO and the nitrosyl group in acidified LBN media.

First, this phenomenon is able to be detected via CV as the production of a peak at −800 mV is indicative of $NO^+/NO^{\bullet}$ as shown previously for related Fe-nitrosyl complexes (22). As observed in the CV experiments in Fig. 3 *A*–*C*, the appearance of a reduction peak at very negative potentials (−800 mV) occurred in the LBN 6.5 plus $NaNO_2$ (Fig. 3*A*) and LBN 6.5 plus AB569 (Fig. 3*C*) conditions. This was not observed in the LBN 6.5 plus EDTA conditions (Fig. 3*B*). Interestingly, AB569 was able to generate a slightly greater peak at −800 mV than $NaNO_2$ alone. This implies a slightly greater production of Fe-($NO^+/NO^{\bullet}$) complexes in AB569 that requires further investigation to determine a role in AB569 treatment.

In contrast, amperometric detection did not indicate a difference in the amount of NO produced regardless if EDTA was present. This was interesting, given the small peak observed before in CV, but it was possible that free NO (detectable by amperometry) did not change, but iron bound (DNIC related) did increase. However, this result prompted the application of a third method, EPR.

The NO spin trap Fe-MGD reacts with NO to produce a unique triplet signal, even at low concentrations. However, as seen in Fig. 3*E*, the AB569 combination failed to produce this signal, while A-NO_2^- clearly did. The lack of EPR signal by AB569 is especially interesting, given that $NaNO_2$ is present and NO generation is still occurring as shown in previous studies of amperometric measurement. This may be due to the absorption effect of Fe-EDTA (both the Fe^{2+} and Fe^{3+} states, discussed below). If the signal of MGD-Fe-NO triggered by $NaNO_2$ is then put into competition with another molecule that binds NO, such as ($Fe^{2+/3+}$)EDTA, it is possible that the signal may be decreased below a detectable threshold. This absorption effect could also explain the increased killing seen in our studies. It has been shown previously that (Fe^{2+})EDTA chelates can be used in aqueous solutions to scrub NO out of the gas phase in industrial chimney flues (33). This process is due to the aqueous (Fe^{2+})EDTA allowing for a greater solubility of NO, which then forces the equilibrium in favor of the aqueous phase (being, in essence, a combination of (Fe^{2+})EDTA-NO and $NO_{(aq)}$) (34).

We believe this absorption is part of the underlying principle behind AB569 treatment. By adding NO_2^- and EDTA to LBN 6.5, several chemical reactions ensue, the first of which is the production of nitrous acid (HONO). HONO is known to be reactive and produce NO via reduction. Previous reports have shown that both NO_2^- and HONO can interact with (Fe^{2+})-EDTA, which oxidizes Fe^{2+} to Fe^{3+} and releases NO and another byproduct (reactions 1, 2, and 3 in *SI Appendix*, Fig. S4) (35). This NO can then interact with another moiety of (Fe^{2+})EDTA, thereby creating a relatively stable (Fe^{2+})EDTA-NO molecule. As a result, for every one molecule of HONO or NO_2^-, two molecules of (Fe^{2+})EDTA will be consumed, leading to concerns about iron limitation. However, it has also been shown that (Fe^{3+})EDTA can also bind NO, albeit much weaker than its Fe^{2+} counterpart, adding additional absorption opportunities to the system (36). Once bound, (Fe^{2+})EDTA-NO and (Fe^{3+})EDTA-NO can release NO into the environment at a slower rate. This could be creating a time release of NO into the media. This also corroborates the killing studies and helps to explain the increased killing without a recovery of CFU over several days. With a traditional single dose NO_2^- treatment, our laboratory has seen that after an initial burst of killing, the culture would begin to recover if left longer (beginning at 2 to 3 d; *SI Appendix*, Fig. S1*A*). This effect has not been seen in AB569-treated cultures (*SI Appendix*, Fig. S1*A*).

Additionally, previous reports have shown that EDTA can prevent the loss of a S-nitrosyl moiety from proteins. This is assumed to be from the loss of available catalytic transition metals from the solution, which slows down the loss of the nitrosyl moiety. This phenomenon was tested with preformed S-Nitrosylated Cysteine (Cys-NO) that was added to LBN 6.5 with or without EDTA. It was seen that the presence of 1 mM EDTA in the media reduced the production of NO by 33%, a significant protective effect (Fig. 4*B*). This protection implies a mechanistic underpinning of AB569 treatment, in that it may be able to both produce and protect SNO proteins, through the $NaNO_2$ and EDTA components, respectively, which could allow for prolonged antimicrobial action through a slower release of NO from these moieties.

Conclusions. The mechanism of action of AB569 is still unclear as neither component is limited to a single pathway, but it is clear that a myriad of effects is occurring. Although this report does present data that the combination can act in a bactericidal manner (Fig. 1 and *SI Appendix*, Fig. S1), this cannot be stated conclusively until the mechanism is elucidated. AB569 causes massive transcriptional dysregulation in *PA*, leading to a loss of vital cellular functions. The combination of A-NO_2^- and EDTA may be increasing the amount of NO, both through the generation and protection of DNIC complexes and *S*-nitrosylated proteins. It is possible that this increase in detectable NO complexes can supply NO to the system over a longer period. If true, this could be interacting with more regulatory elements in the cell, leading to the vast dysregulation seen in the RNA-seq results. Although further investigation is required to discern how these interactions are exactly influencing the bacterial cell, it seems that this combination has the potential to help prevent the growth and kill problematic pathogens.

Materials and Methods

Full materials and methods are available in *SI Appendix* for this manuscript. A summary is listed below.

All strains were grown in either LB or TSB, as indicated, and tested with the same media supplemented with 1% KNO_3 and adjusted to pH 6.5 with 50 mM phosphate buffer. Broth-based killing assays and checkerboard studies were conducted for the indicated amounts of time, after which CFU/mL or OD_{600} was assessed, respectively. Biofilm killing was performed in 96-well plates for 48 h, after which the remaining biofilm was dispersed and subjected to live/dead analysis using a FACSCalibur flow cytometer. RNA sequencing was conducted on anaerobic *P. aeruginosa* PAO1 cells following 3 h of treatment, as indicated. Following RNA purification and library preparation, samples were run on an Illlumina HiSeq2500, and the data were aligned to the PAO1 genome using STAR (Spliced Transcripts Alignment to a Reference). The reads were analyzed using the KEGG database, PseudoCyc metabolic pathway database, and GO term annotations. The variety of human cells used in this study are outlined properly in *SI Appendix* for this manuscript. For the primary human dermal fibroblasts, cells were generously provided by Dr. Zalfa Abdel-Malek (University of Cincinnati, Study 2018-3443, IRB exempt). Other cells used in this study consisted of cell lines. Each cell was maintained in appropriate media for that cell and tested in the same media supplemented with 1% KNO_3 and adjusted to a pH of 6.5 using 50 mM phosphate buffer. Viability testing was conducted on treated cells using a Sytox orange staining protocol and analyzed via a FACSCalibur flow cytometer. In vivo testing was conducted on 6-wk-old Balb/C mice that were infected intratracheally with 2×10^6 CFU of PAO1 embedded in alginate. Twenty-four hours after infection, mice were treated daily for 5 d, after which the lungs were harvested and analyzed. Electrochemical analyses were conducted following standard protocols. Amperometric detection was conducted using an ISO-NOP (World Precision Instruments) with a water jacket to maintain the temperature at 37 °C. CV was performed on a CH Instruments CH-660D electrochemical workstation (22 ± 1 °C), with a three-electrode configuration applied in a cell with a glassy carbon working electrode, Ag/AgCl (3 M KCl, 0.19 V vs. NHE) reference electrode, and graphite counter electrode. EPR was performed on a

JEOL USA, Inc., JES-X310 X-band (9.5 GHz) spectrometer with a TE_{011} cylindrical resonator and degassed quartz capillary sample tubes. Field modulation of 1.0 G was applied for a scan time of 30 s and an output time constant of 0.03 s. For biological assays, a Student's *t* test was performed for statistical significance. For the RNA-sequencing results, significance was confirmed using a hypergeometric analysis confirmed by the Benjamini and Hochberg method. Data are available upon request. The RNA sequencing results have been uploaded to National Center for Biotechnology Information Gene Expression Omnibus database and can be accessed with series entry number GSE142611 (20).

ACKNOWLEDGMENTS. We thank Arch Biopartners, Inc. (Toronto, Canada), for support of this study.

1. S. S. Yoon *et al*., Anaerobic killing of mucoid *Pseudomonas aeruginosa* by acidified nitrite derivatives under cystic fibrosis airway conditions. *J. Clin. Invest.* **116**, 436–446 (2006).
2. T. A. Major *et al*., Sodium nitrite-mediated killing of the major cystic fibrosis pathogens *Pseudomonas aeruginosa*, *Staphylococcus aureus*, and *Burkholderia cepacia* under anaerobic planktonic and biofilm conditions. *Antimicrob. Agents Chemother.* **54**, 4671–4677 (2010).
3. S. Su *et al*., Catalase (KatA) plays a role in protection against anaerobic nitric oxide in *Pseudomonas aeruginosa*. *PLoS One* **9**, e91813 (2014).
4. F. C. Fang, Perspectives series: Host/pathogen interactions. Mechanisms of nitric oxide-related antimicrobial activity. *J. Clin. Invest.* **99**, 2818–2825 (1997).
5. A. R. Richardson, P. M. Dunman, F. C. Fang, The nitrosative stress response of *Staphylococcus aureus* is required for resistance to innate immunity. *Mol. Microbiol.* **61**, 927–939 (2006).
6. E. Banin, K. M. Brady, E. P. Greenberg, Chelator-induced dispersal and killing of Pseudomonas aeruginosa cells in a biofilm. *Appl. Environ. Microbiol.* **72**, 2064–2069 (2006).
7. F. R. Champlin, M. L. Ellison, J. W. Bullard, R. S. Conrad, Effect of outer membrane permeabilisation on intrinsic resistance to low triclosan levels in Pseudomonas aeruginosa. *Int. J. Antimicrob. Agents* **26**, 159–164 (2005).
8. S. Finnegan, S. L. Percival, EDTA: An antimicrobial and antibiofilm agent for use in wound care. *Adv. Wound Care (New Rochelle)* **4**, 415–421 (2015).
9. R. E. Wood, J. D. Klinger, M. J. Thomassen, H. A. Cash, "The effect of EDTA and antibiotics on Pseudomonas aeruginosa isolated from cystic fibrosis patients: A new chemotherapeutic approach" in *Perspectives in Cystic Fibrosis*, J. M. Sturgess, Ed. (Canadian Cystic Fibrosis Foundation, Toronto, 1980), pp. 365–369.
10. H. Downes, C. A. Hirshman, Importance of calcium in citric acid-induced airway constriction. *J. Appl. Physiol.* **55**, 1496–1500 (1983).
11. H. Downes, C. A. Hirshman, Calcium chelators increase airway responsiveness. *J. Appl. Physiol.* **59**, 92–95 (1985).
12. C. R. Beasley, P. Rafferty, S. T. Holgate, Bronchoconstrictor properties of preservatives in ipratropium bromide (Atrovent) nebuliser solution. *Br. Med. J. (Clin. Res. Ed.)* **294**, 1197–1198 (1987).
13. R. D. Coakley *et al*., Abnormal surface liquid pH regulation by cultured cystic fibrosis bronchial epithelium. *Proc. Natl. Acad. Sci. U.S.A.* **100**, 16083–16088 (2003).
14. C. McDaniel *et al*., A putative ABC transporter permease is necessary for resistance to acidified nitrite and EDTA in *Pseudomonas aeruginosa* under aerobic and anaerobic planktonic and biofilm conditions. *Front. Microbiol.* **7**, 291 (2016).
15. G. Orhan, A. Bayram, Y. Zer, I. Balci, Synergy tests by E test and checkerboard methods of antimicrobial combinations against Brucella melitensis. *J. Clin. Microbiol.* **43**, 140–143 (2005).
16. T. Vishwantha *et al*., Antibiotic synergy test: Checkerboard method on multidrug resistant *Pseudomonas aeruginosa*. *Int. Res. J. Pharm.* **2**, 196–198 (2011).
17. M. J. Hall, R. F. Middleton, D. Westmacott, The fractional inhibitory concentration (FIC) index as a measure of synergy. *J. Antimicrob. Chemother.* **11**, 427–433 (1983).
18. J. W. Costerton, Z. Lewandowski, D. E. Caldwell, D. R. Korber, H. M. Lappin-Scott, Microbial biofilms. *Annu. Rev. Microbiol.* **49**, 711–745 (1995).
19. S. S. Yoon *et al*., *Pseudomonas aeruginosa* anaerobic respiration in biofilms: Relationships to cystic fibrosis pathogenesis. *Dev. Cell* **3**, 593–603 (2002).
20. E. Gill, A nontoxic chemical tandem that kills major human pathogenic bacteria. National Center for Biotechnology Information Gene Expression Omnibus. https://www.ncbi.nlm.nih.gov/geo/query/acc.cgi?acc=GSE142611. Deposited 26 December 2019.
21. G. L. Winsor *et al*., Enhanced annotations and features for comparing thousands of Pseudomonas genomes in the Pseudomonas genome database. *Nucleic Acids Res.* **44**, D646–D653 (2016).
22. T. C. Berto *et al*., Structural and electronic characterization of non-heme Fe(II)-nitrosyls as biomimetic models of the Fe(B) center of bacterial nitric oxide reductase. *J. Am. Chem. Soc.* **133**, 16714–16717 (2011).
23. A. F. Vanin, I. V. Malenkova, V. A. Serezhenkov, Iron catalyzes both decomposition and synthesis of S-nitrosothiols: Optical and electron paramagnetic resonance studies. *Nitric Oxide* **1**, 191–203 (1997).
24. A. F. Vanin *et al*., Dinitrosyl-iron complexes with thiol-containing ligands: Spatial and electronic structures. *Nitric Oxide* **16**, 82–93 (2007).
25. A. M. Komarov, D. A. Wink, M. Feelisch, H. H. H. W. Schmidt, Electron-paramagnetic resonance spectroscopy using N-methyl-D-glucamine dithiocarbamate iron cannot discriminate between nitric oxide and nitroxyl: Implications for the detection of reaction products for nitric oxide synthase. *Free Radic. Biol. Med.* **28**, 739–742 (2000).
26. D. A. Wink *et al*., Detection of S-nitrosothiols by fluorometric and colorimetric methods. *Methods Enzymol.* **301**, 201–211 (1999).
27. N. S. Bryan, M. B. Grisham, Methods to detect nitric oxide and its metabolites in biological samples. *Free Radic. Biol. Med.* **43**, 645–657 (2007).
28. F. Dixon *et al*., Treatment with nitric oxide in the neonatal intensive care unit is associated with increased risk of childhood cancer. *Acta Paediatr.* **107**, 2092–2098 (2018).
29. D. A. Wink *et al*., DNA deaminating ability and genotoxicity of nitric oxide and its progenitors. *Science* **254**, 1001–1003 (1991).
30. G. B. Huffnagle, R. P. Dickson, N. W. Lukacs, The respiratory tract microbiome and lung inflammation: A two-way street. *Mucosal Immunol.* **10**, 299–306 (2017).
31. D. N. O'Dwyer, R. P. Dickson, B. B. Moore, The lung microbiome, immunity, and the pathogenesis of chronic lung disease. *J. Immunol.* **196**, 4839–4847 (2016).
32. P. Seth *et al*., Regulation of MicroRNA machinery and development by interspecies S-nitrosylation. *Cell* **176**, 1014–1025.e12 (2019).
33. P. van der Maas, P. van den Brink, S. Utomo, B. Klapwijk, P. Lens, NO removal in continuous BioDeNOx reactors: Fe(II)EDTA2- regeneration, biomass growth, and EDTA degradation. *Biotechnol. Bioeng.* **94**, 575–584 (2006).
34. P. van der Maas, T. van de Sandt, B. Klapwijk, P. Lens, Biological reduction of nitric oxide in aqueous Fe(II)EDTA solutions. *Biotechnol. Prog.* **19**, 1323–1328 (2003).
35. V. Zang, R. Van Eldik, Influence of the polyamino carboxylate chelating ligand (L) on the kinetics and mechanism of the formation of FeII(L)NO in the system FeII(L)/NO/HONO/NO2- in aqueous solution. *Inorg. Chem.* **29**, 4462–4468 (1990).
36. E. Sada, H. Kumazawa, I. Kudo, T. Kondo, Absorption of nitric oxide in aqueous solutions of iron(III)-EDTA chelate and aqueous slurries of magnesium sulfite with iron(III)-EDTA chelate. *Ind. Eng. Chem. Process Des. Dev.* **20**, 46–49 (1981).